

Characterising foliage influence on LoRaWAN pathloss in a tropical vegetative environment

 ISSN 2043-6386
 Received on 24th November 2019
 Revised 23rd March 2020
 Accepted on 9th April 2020
 E-First on 22nd June 2020
 doi: 10.1049/iet-wss.2019.0201
 www.ietdl.org

Margaret Richardson Ansah¹ ✉, Robert A Sowah¹, Joan Melià-Seguí², Ferdinand A Katsriku³, Xavier Vilajosana⁴, Wiafe Owusu Banahene¹

¹Computer Engineering Department, University of Ghana, Accra, Ghana

²Faculty of Computer Science and Telecommunications, Universitat Oberta de Catalunya (UOC), Barcelona, Spain

³Computer Science Department, University of Ghana, Accra, Ghana

⁴Internet Interdisciplinary Institute (IN3), Universitat Oberta de Catalunya (UOC), Castelldefels, Spain

✉ E-mail: magirich@yahoo.co.uk

Abstract: Ubiquitous computing for remote monitoring is enabling the Internet of Things applications in diverse areas. The potential impact of wireless sensor networks in remote habitat and agricultural monitoring cannot be overemphasised. LoRa (long range) is particularly well suited to applications requiring low operational costs, long-range wireless communication technology, low data rates and low power consumption. For industrial and large-scale deployment of this promising technology, it must be both empirically and theoretically evaluated and proven. For network design purposes and optimised positioning of devices, the authors evaluated long range wireless area network (LoRaWAN) propagation in a tropical vegetative environment. Traditional vegetation propagation models have been compared with the measured data. The free space model best fits their data except for the tree canopy area where the loss was about 56 dB. The result can be used as empirical bases to develop an accurate model and simulation tool for LoRaWAN deployment planning.

1 Introduction

As low-power wireless area networks (LPWANs) technologies continue to grow through research and areas of application, the trade-off of cost minimisation and energy efficiency, data rate, and long-range still compete for attention. The suitability of wireless sensor networks (WSNs) for large scale outdoor applications largely depends on the radio link of the network. The dynamics of higher-layer mechanisms such as sensor node deployment, mobility management, routing is determined by the radio link due to the dynamic nature of the outdoor environment. Existing communication technologies especially IEEE 802.15.4 which operates in the 2.4 GHz frequency band, are being challenged with range and interference limitations. Congestion in the 2.4 GHz band causes interference, and high-power consumption in addition to short-range due to high attenuation at higher frequencies [1]. LoRa (long range) [2], which is the modulation scheme, and LoRaWAN [3]: the protocol stack and network architecture, has received much attention from both industry and academia alike due to the capabilities of long-range, low power and low interference makes it suitable for WSN.

Deployment in dense vegetation requires an in-depth understanding of the behaviour of the radio link in such an environment to facilitate large-scale network planning and management. Propagating wireless signals can be affected by various conditions such as the environment, antenna location and height, terrain, distance between the transmitter and receiver [4]. The reduction or distortion of the power density of the signal caused by the effect of these factors is termed path loss. Evaluating the path loss for an environment such as vegetation or foliage inform the design and planning of network for various applications that closely represent the channel in such an environment. LoRaWAN deployment is still early-stage and therefore needs to be proven in a different environment.

Empirical evaluations of LoRaWAN in an urban and suburban environment relatively abound [5–11] as well as that of rural [12, 13], compared to an evaluation in vegetation environment. There are other studies conducted in a foliated environment but are either preliminary for a future detailed study [14] or focused on the

development of the monitoring system [15]. Mobile gateway driven by a drone was used to evaluate LoRaWAN on a tree farm to monitor environmental data [14]. The battery of the drone had to be replaced many times within a day. Thus, defeating the aim of WSN which should be able to work unattended for years.

An implementation of an irrigation system based on LoRaWAN was presented in [16]. The sensors picked ambient temperature, humidity, the wetness of leaf and soil moisture on a vineyard. The evaluation, however, focused on the data analytics service than the performance of the LoRaWAN behaviour on the farm. A review of closely related studies in the vegetation environment is presented in the next section.

This study empirically evaluates LoRaWAN performance in a tropical vegetation environment to understand the behaviour of the radio link in such an environment to facilitate large-scale network planning and management while assessing its suitability for use in WSN application in such an environment.

The rest of the paper is as follows: Section 2 discusses the literature related to the study, followed by an overview of LoRa and vegetation propagation models in Section 3. The procedure for the measurement campaign follows in Section 3. The result is presented and discussed in Section 4 and Section 5 concludes the paper with future work.

2 Related works

There are few works done to characterise the path loss effect on LoRaWAN in foliage deployment. Masadan *et al.* [17], quantified the effect of foliage on signal attenuation and its contribution to path-loss and link budget calculations. The Hata/Okumura, Log-normal shadowing and vegetation propagation models were compared to the measured data. This study was conducted on a university campus and, therefore, does not represent a true vegetation environment as suggested by their choice of the model they compared the measured data with. A channel attenuation and coverage investigation of LoRaWAN was also modelled by Petajajarvi *et al.* [9], using the received signal strength indicator (RSSI) to compare range with signal strength and packet loss ratio.

Their work was conducted in an urban environment and on the sea in a line of sight (LOS). The authors derived path loss exponent from comparing the measured data to the log-distance model. Empirical characterisation of the radio channel for a body-centred LoRaWAN was investigated and modelled mathematically to understand the body-shadowing effect on the radio link was also done in [18]. Catherwood *et al.* found the Nakagami distribution with $\mu=0.52$ to be the best fit model. In [19], the role of topographical data to improve the accuracy of an LPWAN path loss model was evaluated by testing different path-loss models for LoRa and comparing the results to measured data. The experiment was conducted in a sub-urban with different terrain. The authors assessed whether false positives or false negatives are more important for the deployment of an LPWAN and concluded that reducing false positives to improve signal reception was desirable but was expensive. They found no single model that best fit the job, but the ITM model had a balanced ratio of false positives and false negatives and significantly reduced the error in areas with vast elevation differences. Coverage comparison was made in [20] for General Packet Radio Service, Narrowband-Internet of Things (IoT), LoRa, and Sigfox for a 7947 km² area with two different models. The authors showed the coverage capabilities of four different technologies but did not compare the evaluated path-loss models with measured data. The evaluation of vegetation impact on LoRa [21] in a rubber plantation is similar to this study. However, Ahmad *et al.* reported on the received signal for the communication range as a preliminary result of their research with no further data analysis.

Rahman *et al.* [22] implemented a weather station monitoring system using LoRaWAN which passed through vegetation. They found inconsistency in the transmitting power for a very low receive power with mean RSSI of 7.34 dBm instead of 14 dBm. The RSSI decreased by 6.7 dBm for every 1–10 m increase in distance. Suci *et al.* [23] also compared LoRa hardware end devices to estimate IoT devices in terms of scalability. Nordin *et al.* [24] analysed the performance of LoRaWAN for the implementation of a water monitoring system. The communication range was found to be a maximum of 1.3 km.

The impact of different physical layer parameters of the LoRaWAN network in tree farms was analysed by Yim *et al.* [25]. They evaluated the effect of LoRa PHY settings on reliability and coverage of LoRaWAN in a mid-life Maples, Oaks and Pine tree farm spaced 8-feet apart. The spreading factors (SFs), Coding rates and Bandwidth were varied at a transmit power of 13 dBm and a gateway height of 2.5 m above the ground. They established that the radio communication range of LoRaWAN was shorter compared to its performance reported by Semtech [26].

Again an exploratory insight into the behaviour of LoRaWAN in the presence of vegetation and hill was given by Iova *et al.* [27]. A hill of 10–15 m high above the ground surrounded by an open field with scattered shrubs and a vegetative area of about 650 m above sea level with dense foliage on a steep mountain constituted the experimental space. They obtained 1.5 km connectivity range for LOS measurement on a bicycle lane and a reduced communication range from 450–550 m in an LoS environment to 50–90 m in a non-line-of-sight (NLOS) vegetation environment. The packet delivery rate of 80% at 20 dB in an NLOS vegetation environment. They confirmed that vegetation reduced signal strength.

3 Background

3.1 Basics of LoRa and LoRaWAN

LoRa is a chirp spread spectrum (CSS) modulation technology with a wider band of 125, 250, and 500 kHz, where chirp pulses are used to modulate signals. It is the physical layer which enables the long-range communication link. In CSS, a narrow-band signal is spread over a wider-band channel. Data rate and range trade-offs are made using the SF: the higher the SF, the lower the data rate and the longer transmission range and vice versa. It is robust and resilient against interference, multipath and Doppler effect due to the utilisation of the use of coding gain by the frequency-modulated chirps for increased receiver sensitivity. The use of

coding rate parameter to the level of forward error correction for the payload is responsible for LoRa's robustness to interference but prolong the time-on-air (ToA) when the correction has more redundant bits.

LoRaWAN is an LPWAN technology for long-range low-power low-data-rate applications based on the Industrial, Scientific, and Medical frequency band built on top of LoRa which defines the physical layer. It defines the communication protocol and architecture for the network and is said to have extended coverage through 155 dB maximum coupling, reliable and energy efficient. Gateways are used to relay communication between the end devices and the network server in a star-of-stars topology [2, 3, 26, 28].

The end devices are the usually remotely placed sensor/actuators that control the sensing of the information from the environment. The gateways in the network consist of a transceiver concentrator that can decode ten concurrent transmissions. They serve as a relay between the end device and the network server. The network server manages the network through the elimination of duplicate packets, the adaptation of data rates according to link conditions and power level, and scheduling of acknowledgement. In applications that require acknowledgement, the network server determines which gateway to acknowledge a received message when multiple gateways detect a transmission. The message is then sent to the application server to be accessed by the user. Authentication takes place at the application server in cases where over-the-air authentication is used as well as the clustering of end devices into related applications and geographical locations.

3.2 Radio propagation model

To predict the reliability, behaviour and signal strength in an unobstructed line of sight path (LoS) for the transmitter-receiver distance separation of radio propagation, the Friis Free Space path loss (PL_{FS}) equation [29] in decibel (dB) expressed as

$$PL_{FS} = \frac{G_t G_r \lambda^2}{(4\pi d)^2} \quad (1)$$

is used. G_t and G_r being the transmitter and receiver gain respectively, d is the distance between the transmitter and the receiver, $\lambda = c/f$, propagating at a speed of light c , operating at frequency f . It is, however, customary to use the log-normal model, which is a generic form of the Friis equation for an obstructed path between transmitter and receiver. It is computed using (2)

$$PL_{FS}(d) = PL(d_0) + 10\gamma \log\left(\frac{d}{d_0}\right) + X_\sigma \quad (2)$$

where d_0 is a reference distance and X_σ is a zero-mean random variable with σ standard deviation.

However, the dynamics of propagation in foliage is much more complicated because of the different structure of the vegetation such as leaves, branches, trunks and the depth of the vegetation [4, 30] and other factors such as wind, rain, humidity in the environment [4] which cannot be characterised by the Friis equation.

3.3 Empirical vegetation propagation models

The free space model cannot be used to predict channel attenuation in the presence of foliage due to obstruction by tree trunks, branches, and leaves. Propagating signals from a transmitter to a receiver can be distorted by obstacles in the signal path and the medium through which the signal propagates. That may cause the signal to be reflected, diffracted or scattered resulting in signal fading.

To predict the loss of propagating signal in the presence of foliage, vegetative propagation models, otherwise known as path loss (excess attenuation) models, are used. The numerical models proposed for predicting signal attenuation, even though versatile and accurate, are computationally intensive [31] as such empirical models are often employed. Some of the most used empirical path



Fig. 1 Cocoa farm with shade trees



Fig. 2 Dense forest cover

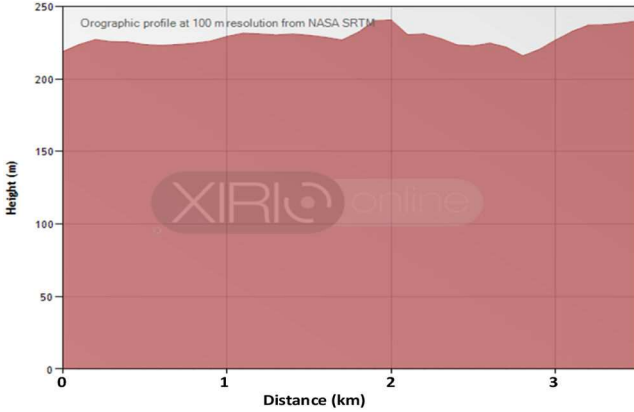


Fig. 3 Elevation profile of farm

Table 1 Tree measurement parameters

Parameter	Cocoa tree, m	Shade tree, m
tree height	3.6	30
trunk height	2	4–35
trunk size	0.4	1.2 and 2.3
branch size	0.1	0.5–4
leaf length	0.29	0.25–0.8
leaf width	0.13	0.11–0.25
ground cover	0.3	1.2
leaf area index	0.27	1.9
tree intervals	3	7.4

loss models are expressed as a function of the signal frequency (f) and the depth of foliage based on the exponential decay model which was proposed by Weissberger [32]. It was modified to produce the modified exponential decay (MED) model which has proven to be coherent in generic attenuation as expressed in (3)

$$PL_{MED} = Xf^Y d^Z \quad (3)$$

where the attenuation due to vegetation PL, at a frequency f , in a vegetation depth of d , X , Y , and Z are constants determined from measured data calculated to result in the best fit in terms of least square error. There are various modified versions, however, since LoRaWAN operates in the sub-GHz frequency band, the ones that

are appropriate for our case are used. This model is suitable for the frequency range from 230 MHz to 95 GHz and for relatively short distance propagation where the signals pass through the vegetation rather than diffract over the tree top [32]. Equation (4) mathematically defines this model

$$PL_W = \begin{cases} 1.33 \times f^{0.284} d^{0.588} & 14m < d < 40m \\ 0.45 \times f^{0.284} d & 0m \leq d < 14m \end{cases} \quad (4)$$

The ITU-R is an empirical vegetation attenuation prediction model applicable for frequencies at 30 MHz to 100 GHz [33]. It predicts attenuation in terms of the frequency of the signal and the depth of the vegetation through which the signal is transmitted with one terminal located in vegetation. The model is expressed in (5)

$$PL_{ITU-R} = 0.2 \times f^{0.3} d^{0.6} \quad (5)$$

where PL is the attenuation due to vegetation in decibel, f is the frequency of the propagating signal, d is the depth of vegetation in meters. ITU-R is reported to give poor fit as the vegetation depth increases due to its prediction of a positive value for the final rate of attenuation curve. This contradicts results from measured data, whose final rate of attenuation has a near-zero gradient [34].

To optimise the ITU-R model for in-leaf and out-of-leaf vegetation, the fitted ITU-R model: obtained from measured data at frequencies of 11.2 and 20 GHz was proposed [35, 34]. Least squared error fit on all measured data was used in the optimisation. The resultant model is defined by (6)

$$PL_{FITU-R} = 0.39 \times f^{0.39} d^{0.25} \quad (6)$$

The COST-235, as defined in (7), is a variant of the ITU-R model for propagation in the vegetation environment

$$PL_{COST235} = \begin{cases} 26.6 \times f^{-0.3} d^{0.5} & \text{out - of - leaf} \\ 15.6 \times f^{-0.009} d^{0.26} & \text{in - leaf} \end{cases} \quad (7)$$

The applicability of the Stanford University Interim models [36, 37], which were defined for Multipoint Microwave Distribution System operating at 2.5 to 2.7 GHz frequency bands, are also tested for LoRaWAN at 868 MHz The type B, as expressed in (8), is the most suitable for our environment as it is characterised by flat terrain, as shown in Fig. 1c, with moderate to heavy tree densities.

$$PL_{SUI} = PL_{FS} + 10\gamma \log_{10} \left(\frac{d}{d_0} \right) + X_h + X_f + s \text{ for } d > d_0 \quad (8)$$

4 Measurement campaign

This section describes the environment and the deployment setup for the measurement campaign to obtain the data, as well as the analysis of the data.

4.1 Environment

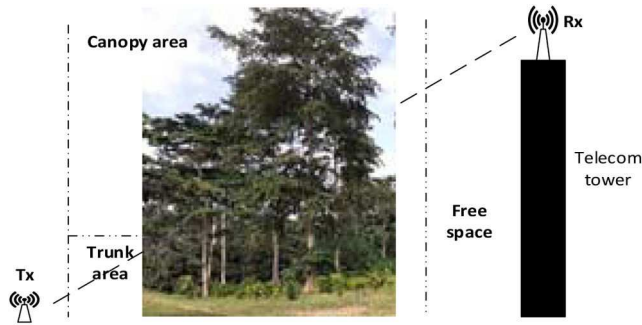
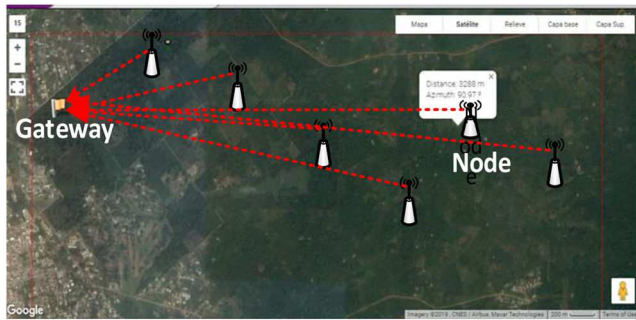
The experiment was conducted at the Cocoa Research Institute of Ghana research farm at Tafo in the Eastern region of Ghana, which is on a flat landform and surrounded by dense semi-deciduous rain forest. A snapshot of the cocoa farm and the forest cover is shown in Figs. 1 and 2 while Fig. 3 presents the orographic profile of the landform.

The research farm and neighbouring farms are 8 km × 4 km with the cocoa plants and a variety of shade trees of the following mean maximum parameters (Table 1):

The farm was planted in between 2007 and 2016, and the trees age ranges between 3 and 13 years old in 2020, while the age of the shade trees ranges from 10 to 50 years old.

Table 2 Measurement parameters settings

Parameter	Value
Frequency, MHz	868
Bandwidth, kHz	125
spreading factor, dBm	7, ..., 12
coding rate	1,2,3,4
transmit Power, dB	14
end device antenna gain, dB	1.5
gateway antenna gain, dBi	5.14
height of LoRa Gateway, m	10,15, 20, 25, 30
height of end device, m	2
clearing distance, m	100

**Fig. 4** Experimental setup B – end node to gateway transmission**Fig. 5** Google map of the environment [40]

4.2 Measuring setup

The end-device is a commercial off-the-shelf STM32 B-L072Z-LRWAN1 discovery board [38] and the TTOG outdoor TTN gateway [39]. The measurement input parameters are shown in Table 2.

The position of the gateway or receiver were static throughout the experiment. The 2 m height of the end device was chosen to be able to pick data from the soil, and the canopy as it also established a radio path through the canopy. At each point, 400 measurements of received signal strength (RSS) values and the signal-to-noise ratio (SNR) were taken. The mean measured values at various intervals were used in the analysis. The test for range and reliability at the same frequency for various distances was done. The data was taken over one month at varied temperature and humidity with the mean ambient temperature of the day were 30°C for hot days and 23°C for normal days and mean humidity of 58 and 80%. The LOS scenario had both the transmitter and receiver placed in a clearing within the farm. In the NLOS scenario, transmitting end devices were placed within the cocoa farm and the receiving gateway is also situated within the farm on a higher elevation above the transmitter with the tree canopy as the obstacle between the transmitter and receiver.

4.3 Data gathering

Measurements were taken at various distances of 50 m interval for NLOS as follows:

Setup A: Two end devices were made to communicate, one as a stationary receiver at the height of 10 and 25 m from the ground. The other acted as a transmitter at 2 m high positioned at 50 m intervals.

Most farming communities have limited or no access to internet service due to their locations close to a forest and away from human settlement. This setup was to evaluate the range of end nodes without a gateway.

Setup B: This setup consists of one gateway at a fixed position of varied heights and seven end devices positioned at various distances from the gateway at the height of 2 m from the ground. The data was sent to the TTN server (Figs. 4 and 5).

Setup C: Fix receiver and a mobile transmitter. The movement mimicked that of grazing and running animals in the farm. The end device, placed at 50 m interval from the stationary gateway, transmitted a payload size of 23 bytes every 30 s continuously without an ACK. The height of the gateway was also varied from 5 to 30 m to test for the best gateway height for long-range.

4.4 Data analysis

The RSSI and the SNR was used to calculate the path loss as in [9]

$$PL_m = |\text{SNR}| + |\text{RSSI}| + P_{tx} + G_{rx} \quad (9)$$

Assuming the path loss exponent and shadow fading standard deviation to be random variables and normally distributed, the log-distance pathloss model in (8) was used to calculate the pathloss exponent while the log-normal pathloss model was used to calculate the shadowing effect of the vegetation on the link.

The expected pathloss, derived from the measured data with a linear and cubic polynomial fit and the rest of the analysis was computed using as in [41, 42]. Replacing the free space path loss $PL(d_0)$ with the measured pathloss PL_m , the equation becomes

$$PL(d) = PL_m + 10\gamma \log\left(\frac{d}{d_0}\right) + X_\sigma \quad (10)$$

The result is compared with established vegetation models to find which best fits measurement.

The regression analyses on the measured data characterise the path loss versus distance, and the data is used to describe these variations statistically. The probability distribution for the measured data was obtained. Using goodness-of-fit tests, inferences based on empirical analysis to verify impacts of possible scenarios on range and reliability and their correlation were made using (11) and the results of the analysis are discussed in the next section

$$\text{RMSE} = \sqrt{\frac{\sum_{i=1}^N (PL_m - \text{EPL})^2}{N}} \quad (11)$$

5 Measurement results and discussion

We analyse the impact of foliage on signal for experimental setup without and with a gateway.

5.1 Comparison with measurements of existing models

We evaluate our result with existing empirical vegetation models, as shown in Fig. 6. For ease of presentation, gateway heights of 10 and 25 m only are presented.

MED model far over-estimate the pathloss of the measured data. This is because MED is suitable for a vegetation depth of 400 m and tends to be incoherent after a vegetation depth of 14 m due to scattering. The FITU-R far underestimates the pathloss of the measured data as shown in Fig. 6.

The measured data present an interesting pattern that cannot be ignored. Attenuation is relatively low at the tree trunk level with a mean of 83 dB at distances <380 m and begins to rise sharply between 400 and 800 m with a maximum mean attenuation of 130

dB. It gradually slows down until at 1 km away from the receiver, and then stabilises with the rate of attenuation is almost negligible. This fluctuation of attenuation with an increase in distance is due to high attenuation at the canopy level and smoothens after the canopy into the open air as shown in Fig. 6. This means that the height of a tree trunk and the canopy depth or size affect the signal.

The best fit model was the Free-space model; however, as the signal passes through the tree canopy, it begins to under-estimate the pathloss. The COST325 fits the data at a distance beyond 1 km.

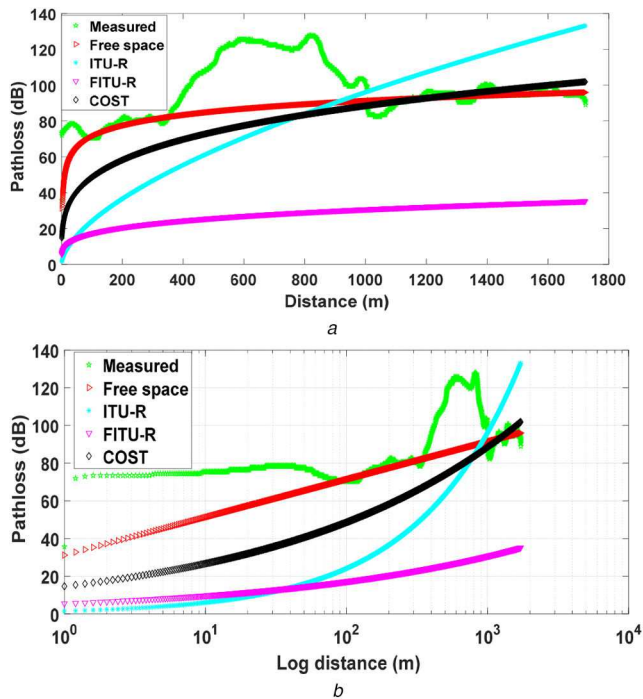


Fig. 6 Comparison of Vegetation models versus (a) Distance, (b) Log-distance, estimation

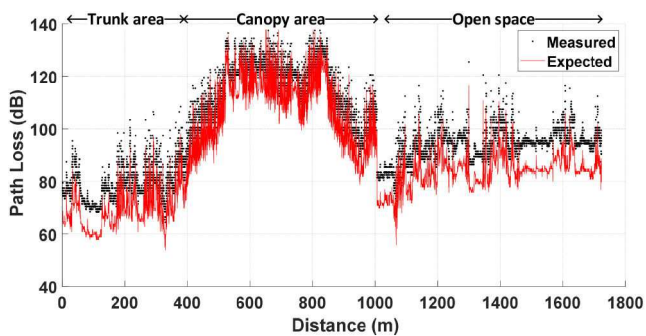


Fig. 7 Comparison of expected and measured pathloss

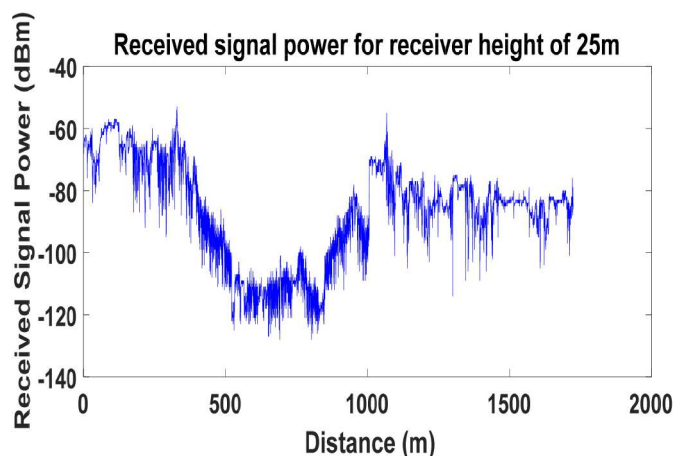


Fig. 8 Measured Received signal power for receiver height of 25 m

The ITU-R underestimated at a distance shorter than 1 km but provided better estimates at a longer distance. It can be observed from Fig. 6 that the measured data pathloss is far higher than the free space path loss by 56 dB between 400 m and 1 km away from the receiver but closes in with an increase in distance. This means that the signal travels through much vegetation to get to the gateway when there is a shorter transmitter-receiver distance separation as can be seen in Figs. 6 and 7.

5.2 Signal coverage

The overall expected signal power was computed as in [43] and compared with the measured received power in Fig. 8.

The distance at which the receiver received a signal from the transmitter was used to determine the range of the network. The network reliability was inferred from the distance at which the packet was received. Reliable data was received with the highest signal strength of -49 dBm and as low as -127 dBm at an SNR of -43 to 27 dB, respectively. For a transmitter height of 2 m and a receiver height of 25 m, a communication range of about 1.75 km was reached. The signal strength over distance for the environment is the same for different receiver heights as can be observed in Fig. 8 and 9. The overall expected signal power was computed as in [43] and compared with the measured received power in Fig. 10.

Similarly, the expected received signal power was computed and compared with measured received signal power is presented in Fig. 11. The expected received signal power in both heights was observed to be lower than the measured values. However, the higher receivers recorded high received signal power and vice versa. As shown in Figs. 8 and 9, the received signal power is weakest at the canopy level. This means that at lower receiver height, the signal passes through much canopy for longer distance to reach the receiver as can be observed in Figs. 9 and 12.

The SNR shows the link performance as the distance increases. As can be observed in Fig. 12, the quality of the link is almost constant at 25 to 27 dB for distances closer to the transmitter (up to 180 m) but sharply deteriorates as distance increases to -43 dB. High receiver height in Fig. 13, however, recorded SNR that is

within the theoretical LoRa range of -20 dB and $+10$ dB. The link quality was the poorest at the tree canopy level. However, it did not impact the packet reception if a signal is received because LoRa can receive signals whose power is 20 dB below the noise floor [26].

In dense vegetation as in Fig. 1, the received signal power for a particular SNR presents an interesting insight of LoRa performance in a harsh environment. The scattered signal, caused by the tree trunk and canopy, reached the receiver at different signal strength as shown in Figs. 14 and 15.

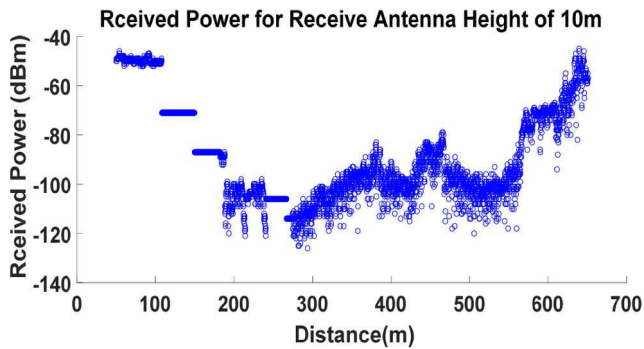


Fig. 9 Mean received power for receiver height of 10 m

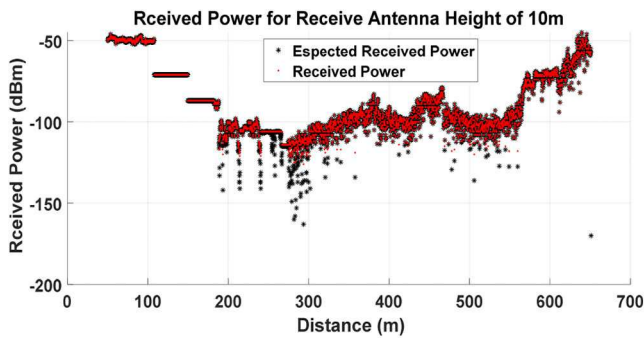


Fig. 10 Comparison of measured and expected received power at receiver height of 25 m

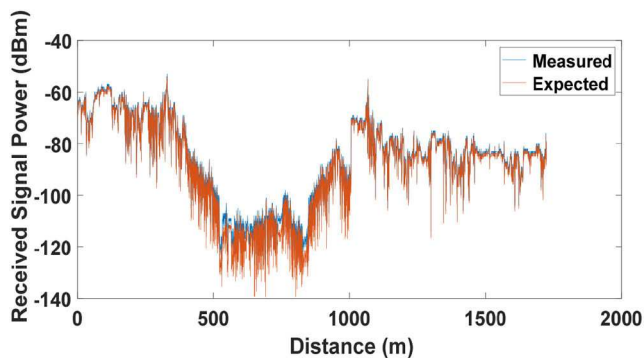


Fig. 11 Measured versus expected received power for receiver height of 10 m

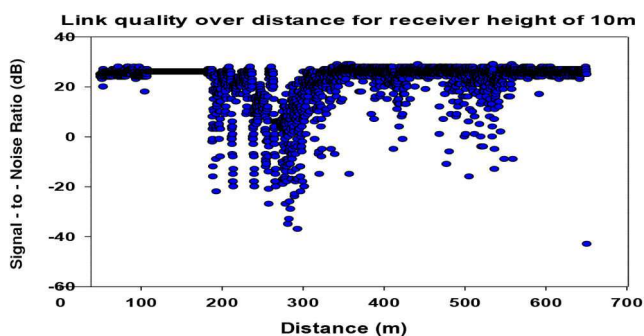


Fig. 12 Distance impact on SNR

5.3 Impact of foliage on the signal with gateway

As expected, the gateway reached further distance for the same height, as can be seen in Fig. 16. In comparison with the values taken without gateway, the highest received signal for the gateway was 50 dB lower than the highest recorded without gateway for the same environment. Another observation is that the difference in the measured and expected received signal power was much more significant for the measurement with gateway than without gateway as can be seen in Figs. 10, 11 and 17. The error margin

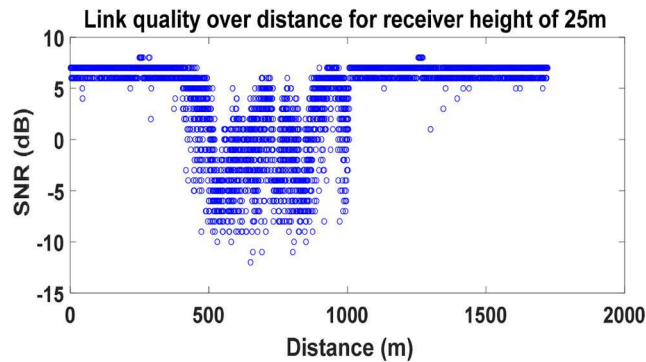


Fig. 13 SNR versus received power at gateway height of 25 m

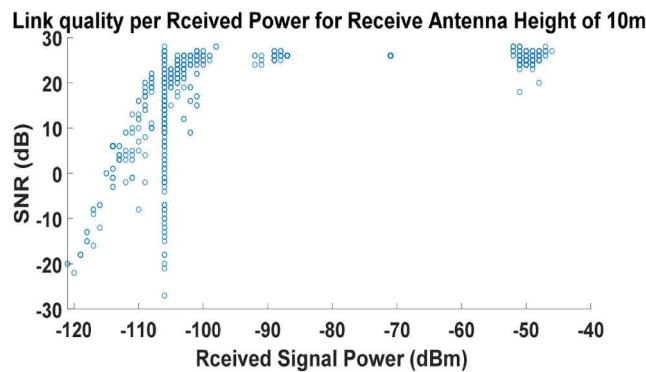


Fig. 14 SNR versus received power at receiver height of 10 m

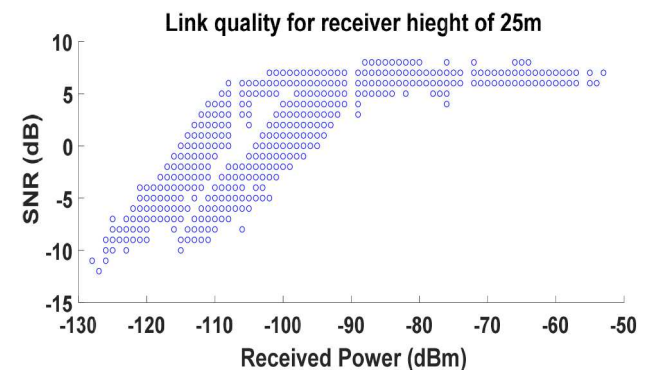


Fig. 15 Link quality for receiver height of 25 m

between measured and expected received signal power (Fig. 17) improves significantly above -120 dBm for setup with gateway.

It can also be observed that increasing receiver heights improved the link quality for receiver height of 10 and 25 m, respectively, as shown in Figs. 12, 13 and 18. Unlike the transmission without gateway, the SNR from the transmission with gateway falls within the typical LoRa range of SNR values of -20 dB and $+10$ dB as shown in Fig. 18.

There was, however, no difference between the reliability of set up with and without a gateway. Fig. 19 confirms the pattern seen in Figs. 14 and 15 that at the canopy level, the signal reaches the gateway with different received power for the same SNR due to scattering. Fig. 20 and Figs. 21–24 show the 3D results of the relationship between parameters such as the received signal power, signal-to-noise ratio, the SF energy consumed and the ToA.

The general energy consumed for received signal power, distance, transmission duration and the corresponding SF used is presented in Figs. 24–27. Notably, the received power at the canopy area was much lower, and higher SFs were used. It, therefore, followed that the energy consumed depends on the SF used and hence the received signal power. As expected in Fig. 27, shorter transmission duration used less energy.

The locations where received power was low, mostly recorded higher SFs irrespective of the distance from the gateway. These findings are opposed to the finding in [5, 44], where the authors

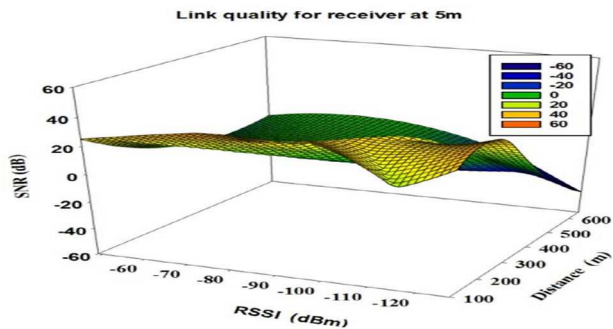


Fig. 16 Communication range and signal power of gateway in vegetation at 25 m

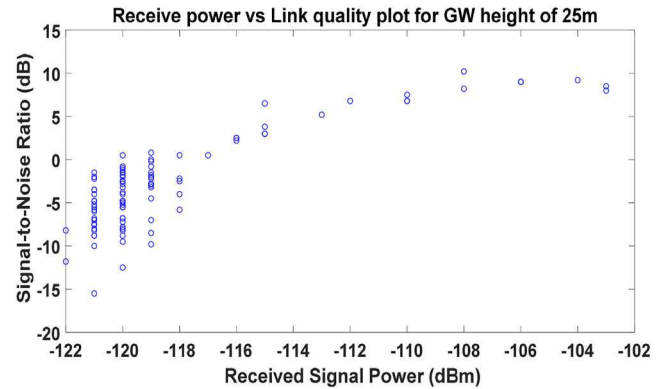


Fig. 20 3D presentation of SNR versus received signal power over distance

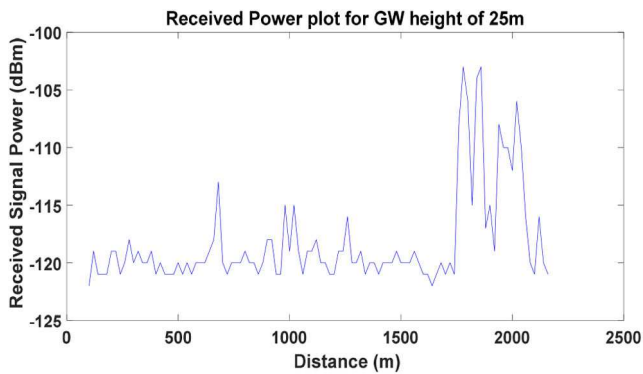


Fig. 17 Comparison of measured and expected range and signal power of gateway in vegetation at 25 m

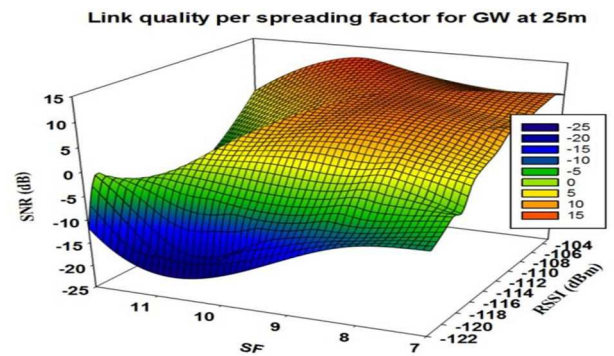


Fig. 21 Link quality per SF and received power

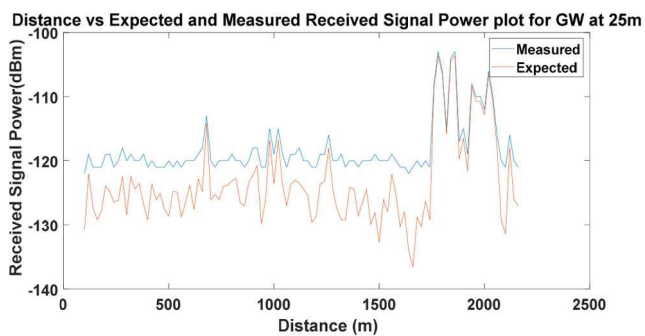


Fig. 18 SNR versus distance plot

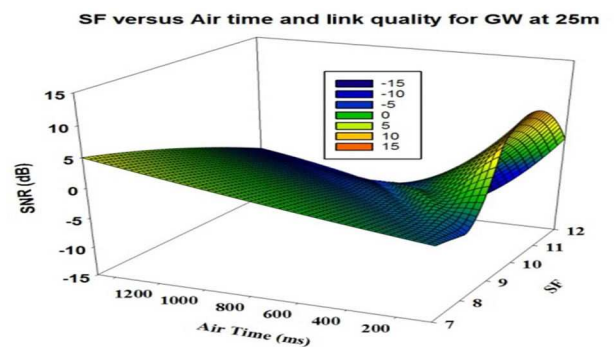


Fig. 22 Link quality per transmission duration and SF

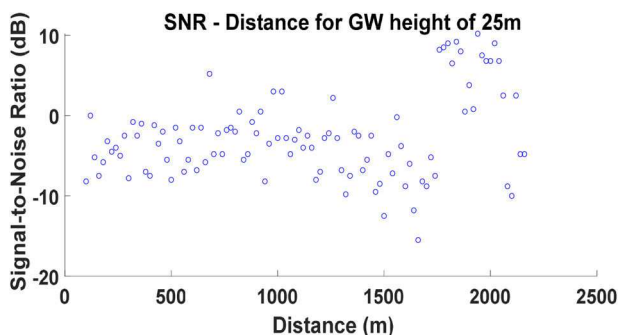


Fig. 19 SNR as a function of distance for GW height of 25 m

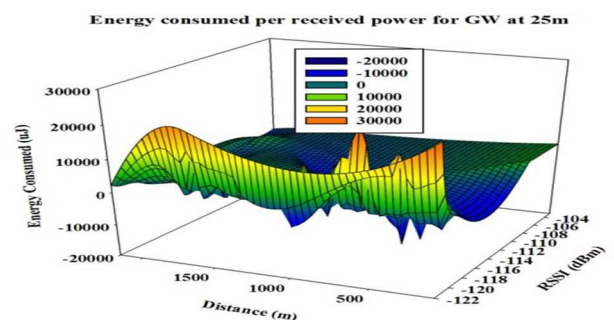


Fig. 23 Energy consumption over distance and received power

found that higher the SF produces higher the reliability. Our findings support the theory that a high value of SF results in lower minimum receiver sensitivity [43, 45]. It can be observed in Fig. 28 that SF12 was used in areas where the received power was weak between -12 and -122 dBm.

Contrary to theory [26] that high SF produces more extended range, our environment showed SF8 and SF9 had the longest range while SF12 gave as short as 300 m as shown in Fig. 29. These results also differ from the findings from an LoS measurement campaign in [46]. The impact of distance on ToA, SF, and SNR

show that the ToA in vegetation propagation follows the theory. Theoretically, the transmission duration doubles at each increase in SF. It, therefore, followed that high SF had longer ToA, as shown in Fig. 30.

Fig. 31 compares the measured ToA with the theoretical ToA calculated using an online tool LoRaTools [47]. The measured ToA was found to be shorter than the calculated ToA. This could mean that the parameters used to calculate ToA in the online tool was for

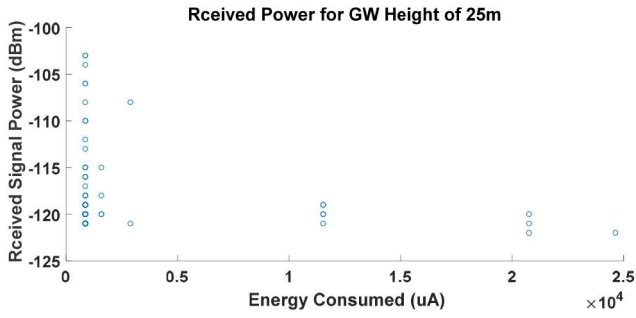


Fig. 24 Energy consumption per received signal power

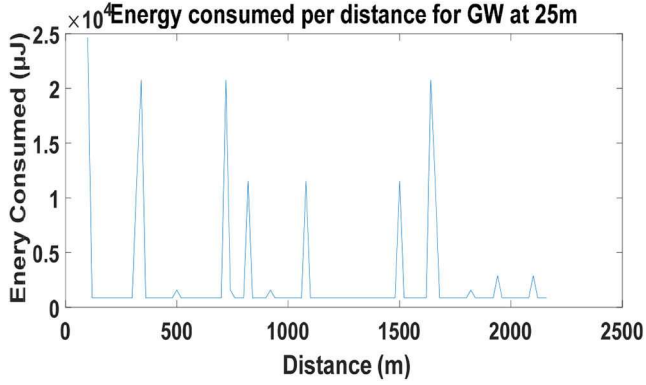


Fig. 25 Energy consumption per distance

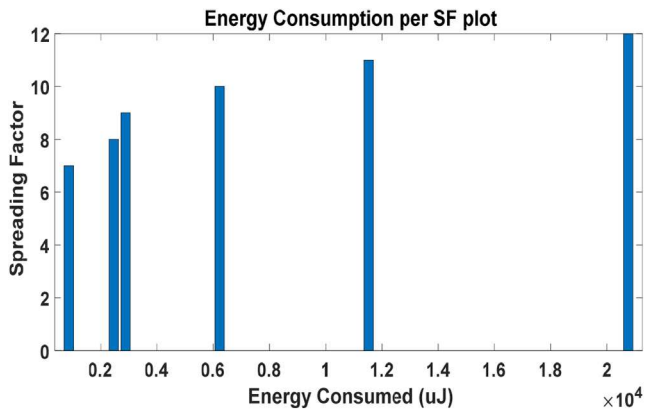


Fig. 26 Energy consumption per spreading power

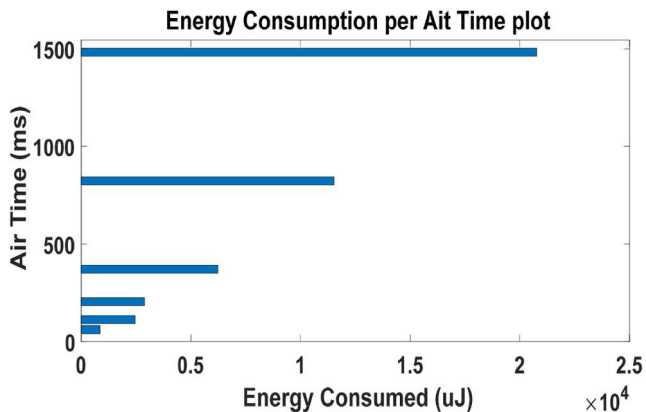


Fig. 27 Energy consumed over transmission duration

either a worst-case scenario or for a different environment other than vegetation.

Another observation is that an increase in SF widens the ToA difference measured and calculated time. This supports the theory that a high SF value results in longer packet transmission but easily decodable signals [3]. The packet duration of the transmitted signal

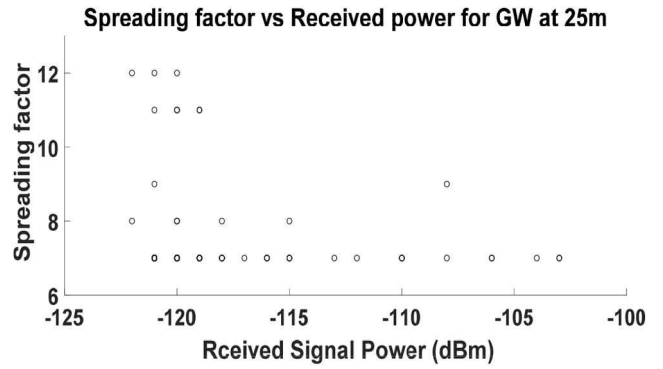


Fig. 28 Relationship between received signal power and SF

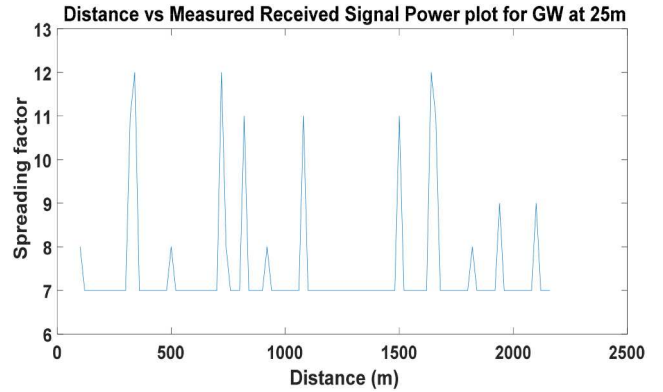


Fig. 29 Relationship between SF and distance

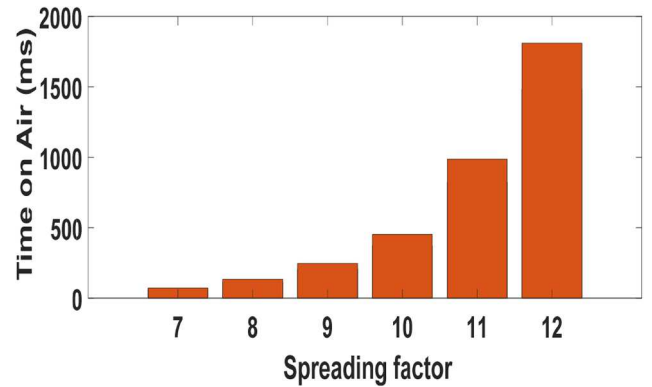


Fig. 30 Relationship between ToA and SF

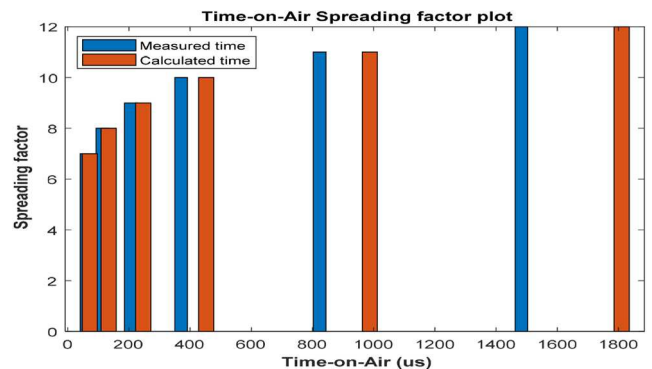


Fig. 31 SF versus measured and calculated airtime

follows the LoRaWAN theory as specified by Yim *et al.* [25], as shown in Fig. 27. The higher SF has the highest time on air.

5.4 General link performance

Overall, the packet delivery rate in all setups was generally good at all receiver heights and communication range which is consistent with the finding in [27].

A maximum of 64 bytes payload size used in this experiment because the application requires the transmission of a few bytes of physical quantities such as temperature, humidity, and soil properties. At all distances and receiver heights where the signal was received, packet reception was about 95% except for receiver height of 10 m where there was 100% packet drop due to a small valley in the farm between distances 2 and 3 km as shown in Fig. 3.

Although minimising range to increase data rate has been proposed in [6], for cost-effective deployment in non-critical applications, long-range is preferred.

6 Conclusion and future work

Coverage and reliability performance measurements were conducted with and without a gateway. LoRaWAN has shown to be robust in the presence of vegetation and can achieve about 3 km for a receiver height of 25 m. We have demonstrated that LoRa performs quite differently in the presence of vegetation. Received signal power that is lower than the minimum threshold of -120 dB was recorded more than 2 dB with gateway and 10 dB without gateway respectively. Its robustness and reliability in the presence of environmental factors such as temperature and humidity coupled with long-range make it an excellent choice for agrarian and other applications in such an environment. For large scale applications, the communication range achieved without gateway will be useful in applications such as ours where there is no internet access to the gateway in most cocoa farms, which are normally situated in dense vegetation environments. Scaling up the network is manageable as a single LoRaWAN gateway has a capacity for up to 10,000 end devices. The reliability achieved also makes its application to tracking wildlife promising. Our findings show that the use of LoRa technology as an alternative radio in WSN can reduce network cost as there is no spectrum and license cost, as well as low deployment cost as a limited number of nodes, is required to cover a wide area. Operational costs such as maintenance will be minimal if end devices are self-healing and self-configuring. In addition to being low power, its long-range capability provides point to point coverage without relay nodes, thus, reducing the cost of energy for end devices.

The result is a preliminary to a broader characterisation of LoRa in vegetation. We are working on characterising the impact of environmental factors on LoRa in vegetation. The next step is to model the propagation result to be included in the LoRa network simulation tool for the environment under study.

7 Acknowledgment

The authors acknowledge the WINE Research Laboratory of the IN3 Group at the University Oberta de Catalona for their support.

8 References

- [1] Doherty, L., Simon, J., Watey, T.: 'Wireless sensor network challenges and solutions', *Microw. J.*, 2012, **55**, (8), pp. 22–34
- [2] Semtech Corporation, A.: 'An1200.22 LoRa™ modulation basics, application note', May 2015: Accessed 15 August 2017
- [3] Alliance, L.: 'A Technical Overview of LoRa and LoRaWAN', White Paper, 2015
- [4] Savage, N., Ndzi, D., Seville, A., *et al.*: 'Radio wave propagation through vegetation: factors influencing signal attenuation', *Radio Sci.*, 2003, **38**, (5), pp. 4–6
- [5] Aref, M., Sikora, A.: 'Free space range measurements with semtech lora™ technology'. 2014 2nd Int. Symp. on Wireless Systems within the Conf. on Intelligent Data Acquisition and Advanced Computing Systems: Technology and Applications (IDAACS-SWS), 2014
- [6] Cattani, M., Boano, C.A., Römer, K.: 'An experimental evaluation of the reliability of lora long-range low-power wireless communication', *J. Sens. Actuator Netw.*, 2017, **6**, (2), p. 7
- [7] Haxhibeqiri, J., Karaagac, A., Van den Abeele, F., *et al.*: 'Lora indoor coverage and performance in an industrial environment: case study'. 2017 22nd IEEE Int. Conf. on Emerging Technologies and Factory Automation (ETFFA), Limassol, Cyprus, 2017
- [8] Petrić, T., Goessens, M., Nuaymi, L., *et al.*: 'Measurements, performance and analysis of lora fabian, a real-world implementation of lpwan'. 2016 IEEE 27th Annual Int. Symp. on Personal, Indoor, and Mobile Radio Communications (PIMRC), IEEE, Valencia Spain, 2016
- [9] Petajarvi, J., Mikhaylov, K., Roivainen, A., *et al.*: 'On the coverage of LPWANs: range evaluation and channel attenuation model for lora technology'. 2015 14th International Conference on ITS Telecommunications (ITST), 2015
- [10] Sanchez-Gomez, J., Gallego-Madrid, J., Sanchez-Iborra, R., *et al.*: 'Performance study of LoRaWAN for smart-city applications'. 2019 IEEE 2nd 5G World Forum (5GWF), Dresden, Germany, 2019
- [11] Sanchez-Gomez, J., Sanchez-Iborra, R., Skarmeta, A.: 'Transmission technologies comparison for IoT communications in smart-cities'. GLOBECOM 2017–2017 IEEE Global Communications Conf., (IEEE, Marina Bay Sands, Singapore, 2017
- [12] Sanchez-Iborra, R., Sanchez-Gomez, J., Ballesta-Viñas, J., *et al.*: 'Performance evaluation of lora considering scenario conditions', *Sensors*, 2018, **18**, (3), p. 772
- [13] Catherwood, P.A., Little, M., Finlay, D., *et al.*: 'Recovery of incapacitated commercial delivery drones using LPWAN technology', *IEEE Intell. Transp. Syst. Mag.*, 2019, **12**, (2), pp. 6–19
- [14] Park, S., Yun, S., Kim, H., *et al.*: 'Forestry monitoring system using lora and drone'. Proc. of the 8th Int. Conf. on Web Intelligence, Mining and Semantics, Novi Sad, Serbia, 2018
- [15] Kadir, E.A., Efendi, A., Rosa, S.L.: 'Application of lora wan sensor and IoT for environmental monitoring in Riau province Indonesia', *Proc. Electr. Eng. Comput. Sci. Inf.*, 2018, **5**, (5), pp. 281–285
- [16] Daveev, D., Mitreski, K., Trajkovic, S., *et al.*: 'IoT agriculture system based on lorawan'. 2018 14th IEEE Int. Workshop on Factory Communication Systems (WFCS), Imperia, Italy, 2018
- [17] Masadan, N.A.B., Habaebi, M.H., Yusoff, S.H.: 'Lora LPWAN propagation channel modelling in IIUM campus'. 2018 7th Int. Conf. on Computer and Communication Engineering (ICCCCE), Liverpool, U.K., 2018
- [18] Catherwood, P., McComb, S., Little, M., *et al.*: 'Channel characterisation for wearable lorawan monitors', 2017
- [19] Linka, H., Rademacher, M., Aliu, O.G., *et al.*: 'Path loss models for low-power wide-area networks: experimental results using lora', 2018
- [20] Lauridsen, M., Nguyen, H., Vejlgard, B., *et al.*: 'Coverage comparison of GPRS, NB-IoT, lora, and sigfox in a 7800 Km² area'. Vehicular Technology Conf. (VTC Spring), 2017 IEEE 85th, Sydney, Australia, 2017
- [21] Ahmad, K.A., Salleh, M.S., Segaran, J.D., *et al.*: 'Impact of foliage on lora 433MHz propagation in tropical environment'. AIP Conf. Proc., Maharashtra, India, 2018
- [22] Rahman, N.A., Yamada, Y., Husni, M., *et al.*: 'Analysis of propagation link for remote weather monitoring system through lora gateway'. 2018 2nd Int. Conf. on Telematics and Future Generation Networks (TAFGEN), TBA, Malaysia, 2018
- [23] Suci, G., Petrache, A.L., Badea, C., *et al.*: 'Low-power IoT devices for measuring environmental values'. 2018 IEEE 24th Int. Symp. for Design and Technology in Electronic Packaging (SIITME), Iași, Romania, 2018
- [24] Nordin, R., Mohamad, H., Behjati, M., *et al.*: 'The world-first deployment of narrowband IoT for rural hydrological monitoring in unesco biosphere environment'. 2017 IEEE 4th Int. Conf. on Smart Instrumentation, Measurement and Application (ICSIMA), Songkhla, Thailand, 2017
- [25] Yim, D., Chung, J., Cho, Y., *et al.*: 'An experimental lora performance evaluation in tree farm'. Sensors Applications Symp. (SAS), 2018 IEEE, Seoul, Republic of Korea 2018
- [26] Sornin, N., Semtech, L.M.S., Eirich, T. (IBM), *et al.*: 'lorawan specification', 2016, July, Version 1.02
- [27] Iova, O., Murphy, A.L., Picco, G.P., *et al.*: 'Lora from the city to the mountains: exploration of hardware and environmental factors'. Proc. of the 2nd Int. Workshop on New Wireless Communication Paradigms for the Internet of Things (MadCom), Uppsala, Sweden, 2017
- [28] Adelantado, F., Vilajosana, X., Tuset-Peiro, P., *et al.*: 'Understanding the limits of lorawan', *IEEE Commun. Mag.*, 2017, **55**, (9), pp. 34–40
- [29] Friis, H.T.: 'The free space transmission equation', *Proc. IRE.*, 1946, **34**, p. 254
- [30] Barclay, L.: 'Propagation of Radiowaves-2nd Edition', The Institution of Electrical Engineers, 2003
- [31] Arshad, K., Katsriku, F., Lasebae, A.: 'Radiowave vhf propagation modelling in forest using finite elements'. 2006 2nd Int. Conf. on Information & Communication Technologies, Tehran, Iran, 2006
- [32] Weissberger, M.A.: 'An initial critical summary of models for predicting the attenuation of radio waves by trees'. Electromagnetic Compatibility Analysis Center, Annapolis MD, 1982
- [33] ITU, I.-R.R.S.o.: 'Attenuation in vegetation', pp. itu-r 833–839, 2016
- [34] Seville, A., Craig, K.: 'Semi-empirical model for millimetre-wave vegetation attenuation rates', *Electron. Lett.*, 1995, **31**, (17), pp. 1507–1508
- [35] Al-Nuaymi, M.O., Stephens, R.B.L.: 'Measurements and prediction model optimisation for signal attenuation in vegetation media at centimetre wave frequencies', *IEE Proc. Microw. Antennas Propag.*, 1998, **145**, (3), pp. 201–206
- [36] Erceg, V., Greenstein, L.J., Tjandra, S.Y., *et al.*: 'An empirically based path loss model for wireless channels in suburban environments', *IEEE J. Sel. Areas Commun.*, 1999, **17**, (7), pp. 1205–1211
- [37] Hari, K., Baum, D., Rustako, A., *et al.*: 'Channel models for fixed wireless applications', IEEE 802.16 Broadband wireless access working group, 2003
- [38] STMicroelectronics: 'Stm32 B-L072z-Lrwan1 discovery board', <https://www.st.com/en/evaluation-tools/b-l072z-lrwan1.html>
- [39] Network T.T., <https://www.thingsnetwork.org/docs/gateways/thethingsoutdoor/>, 2019

- [40] Maps G., <https://www.google.com/maps/@6.229553,-0.3623211,256m/data=!3m1!1e3>
- [41] Miranda, J., Abrishambaf, R., Gomes, T., *et al.*: 'Path loss exponent analysis in wireless sensor networks: experimental evaluation'. 2013 11th IEEE Int. Conf. on Industrial Informatics (INDIN), London, U.K, 2013
- [42] Mestre, P., Ribeiro, J., Serodio, C., *et al.*: 'Propagation of IEEE802. 15.4 in vegetation'. Proc. of the World Congress on Engineering 2011, 2011
- [43] Demetri, S., Zúñiga, M., Picco, G.P., *et al.*: 'Automated estimation of link quality for lora: a remote sensing approach'. 2019 18th ACM/IEEE Int. Conf. on Information Processing in Sensor Networks (IPSN), Montreal, QC, Canada, 2019
- [44] Boano, C.A., Cattani, M., Römer, K.: 'Impact of temperature variations on the reliability of lora', 2018
- [45] Bor, M., Vidler, J.E., Roedig, U.: 'Lora for the internet of things', 2016
- [46] Ahmad, K., Segaran, J., Hashim, F., *et al.*: 'Lora propagation at 433 MHz in tropical climate environment', *J. Fundam. Appl. Sci.*, 2017, 9, (3S), pp. 384–394
- [47] LoRaTools: <https://www.loratoools.nl/#airtime>